Original article

SARS-CoV-2 Spike protein promotes hyper-inflammatory response that can be ameliorated by Spike-antagonistic peptide and FDA-approved ER stress and MAP kinase inhibitors *in vitro*

Alan C-Y. Hsu[1,2 †], Guoqiang Wang[3], Andrew T. Reid[1,2], Punnam Chander. Veerati[1,2], Prabuddha S. Pathinayake[1,2], Katie Daly[1,2], Jemma R. Mayall[1,2], Philip M. Hansbro[4,5], Jay C. Horvat[1,2], Fang Wang[3], and Peter A. Wark[1,2,6].

[1] Priority Research Centre for Healthy Lungs, The University of Newcastle, Newcastle, New South Wales 2305, Australia

[2] Viruses, Infection / Immunity, Vaccines and Asthma, Hunter Medical Research Institute, Newcastle, New South Wales 2305, Australia

[3] Department of Pathogen Biology, College of Basic Medical Science, Jilin University, Changchun 130021, China.

[4] School of Life Sciences, University of Technology Sydney, New South Wales 2007, Australia

[5] Centenary UTS Centre for Inflammation, Centenary Institute, New South Wales 2050, Australia

[6] Department of Respiratory and Sleep Medicine, John Hunter Hospital, Newcastle, New South Wales 2305, Australia

[†] Correspondence: Dr Alan Hsu, Ph.D.
Priority Research Centre for Healthy Lungs, Hunter Medical Research Institute, Lot 1 Kookaburra Circuit, New Lambton Heights, Newcastle, NSW 2305, Australia.
Email: Alan.Hsu@newcastle.edu.au.

The authors have declared that no conflict of interest exists.

Summary

SARS-CoV-2 infection causes an inflammatory cytokine storm and acute lung injury. Currently there are no effective antiviral and/or anti-inflammatory therapies. Here we demonstrate that 2019 SARS-CoV-2 spike protein subunit 1 (CoV2-S1) induces high levels of NF-κB activations, production of pro-inflammatory cytokines and mild epithelial damage, in human bronchial epithelial cells. CoV2-S1-induced NF-κB activation requires S1 interaction with human ACE2 receptor and early activation of endoplasmic reticulum (ER) stress, and associated unfolded protein response (UPR), and MAP kinase signalling pathways. We developed an antagonistic peptide that inhibits S1-ACE2 interaction and CoV2-S1-induced productions of pro-inflammatory cytokines. The existing FDA-approved ER stress inhibitor, 4-phenylburic acid (4-PBA), and MAP kinase inhibitors, trametinib and ulixertinib, ameliorated CoV2-S1-induced inflammation and epithelial damage. These novel data highlight the potentials of peptide-based antivirals for novel ACE2-utilising CoVs, while repurposing existing drugs may be used as treatments to dampen elevated inflammation and lung injury mediated by SARS-CoV-2.

Keywords:

SARS-CoV-2, COVID-19, Coronavirus, Inflammation, Endoplasmic Reticulum stress

Introduction

The emergence of a novel SARS-coronavirus in late 2019 (SARS-CoV-2; previously known as 2019-nCoV), and the CoV disease (COVID)-19 it causes, has led to a devastating pandemic of the 21st century. SARS-CoV-2 belongs to the beta-coronavirus genus with approximately 79.5% sequence homology to the SARS-CoV that emerged in 2002 (Wang et al., 2020b). Similar to SARS-CoV (2002), this novel CoV also utilises angiotensin converting enzyme (ACE)2 as its host receptor to mediate membrane fusion and virus entry and viral replication (Zhou et al., 2020). SARS-CoV-2 spike protein contains two subunits, subunit 1 (S1) and S2, that mediates viral attachment to ACE2 and membrane fusion, respectively. The receptor-binding domain (RBD) of S1 is the critical region of the spike protein for ACE2 binding.

Human bronchial epithelial cells are both susceptible and permissive to CoV infection and replication, and the innate immune responses produced by which are critical in the early containment of infection and spread. Viral infection results in the activations of several pattern recognition receptors (PRRs) including retinoic acid-inducible gene I like receptors (RLRs; RIG-I and melanoma differentiation associated protein 5 (MDA-5))(Hayman et al., 2019; Saito and Gale, 2008), and toll-like receptors (TLRs; TLR3 and TLR7)(Alexopoulou et al., 2001; Diebold et al., 2004; Le Goffic et al., 2007). Recognition of viral RNAs by these PRRs leads to activation of transcription factor nuclear factor kappa-light-chain-enhancer of activated B cells (NF-κB), which facilitates the expression of pro-inflammatory cytokines such as interleukin (IL)-6 and IL-1β. These cytokines recruit and activate important immune cells including macrophages and neutrophils, which further promote inflammation and contain viral spread (Guan et al., 2020) (Wang et al., 2008). Patients with severe COVID-19 have been shown to have develop enhanced systemic inflammatory responses (aka. cytokine storm), and acute lung injury and acute respiratory distress syndrome (ARDS) (Huang et al., 2020; McGonagle et al., 2020; Mehta et al., 2020). This storm is characterised by heightened levels of IL-6, tumor necrosis factor-α (TNF-α), and C-C motif chemokine ligand (CCL)2. Currently there are no specific antiviral drugs available or anti-inflammatory drugs that have been shown to influence clinical outcomes for people with COVID-19. A broad-spectrum antiviral drug remdesivir is currently being used for COVID-19 through compassionate use requests as well as in clinical trials in the US and China. The anti-malarial drug hydroxychloroquine is also under several clinical trials, although preliminary reports have not shown beneficial effects (Magagnoli et al., 2020; Mahevas et al., 2020).

Here we demonstrate that the SARS-CoV-2 spike protein S1 (CoV2-S1) or RBD (CoV2-RBD) alone stimulates more pronounced production of pro-inflammatory cytokines as well as factors associated with epithelial damage, compared with the S1 and RBD of SARS-CoV (CoV-S1 and -RBD, respectively). This heightened inflammatory response requires S1 and ACE2 interaction and is primarily driven by early endoplasmic reticulum (ER) stress and its adaptive unfolded protein response (UPR), as well as activation of mitogen-activated protein (MAP) kinase signalling pathways. The early induction of ER-UPR results in activation of MAP kinase, and both pathways synergistically leads to NF-κB activation and production of the pro-inflammatory cytokines IL-6, IL-1β, TNF□, and CCL2, the latter three of which have all been shown to contribute to acute lung injury(Kolb et al., 2001) (Sheridan et al., 1997).

Since CoV2-S1 induces NF-κB activation *via* its interaction with ACE2 and early activations of ER-UPR and MAP kinase signallings, we designed a series of CoV2-S1-antagonistic peptides and identified a peptide, designated AP-6, that inhibits S1-ACE2 interaction. We show that CoV2-S1-mediated inflammatory response are not only ameliorated by AP-6, but the heightened inflammatory responses are also inhibited by an FDA-approved ER stress inhibitor 4-phenylbuic acid (4-PBA), and MAP kinase inhibitors trametinib (GSK1120212) and ulixertinib (BVD-523).

Taken together, these data shed light on how the spike protein of SARS-CoV-2 may contribute to the exaggerated inflammatory responses and pathology observed in those with severe COVID-19. The specific antagonistic peptide that specifically target S1 may serve as an antiviral against SARS-CoV-2. We also showed how existing, pathway specific, FDA-approved drugs could be re-purposed and immediately deployed to reduce infection-induced symptoms and pathologies that are primarily driven by exaggerated inflammatory responses.

Results

SARS-CoV-2 spike protein S1 and RBD induces elevated induction of pro-inflammatory responses.

To investigate if SARS-CoV-2 spike protein induces production of pro-inflammatory cytokines, we used a minimally immortalised human bronchial epithelial cell line BCi-NS1.1, which was derived from human primary bronchial epithelial cells (Hayman et al., 2019; Hu et al., 2019; Kedzierski et al., 2017; Walters et al., 2013). BCi-NS1.1 was stimulated with histidine (His)-tagged CoV2-S1, CoV2-RBD, or CoV-S1 or CoV-RBD. Both S1 and RBD of CoV2 induced robust and similar levels of pro-inflammatory cytokines (IL-6, IL-1β, and TNF) in a dose-dependent manner at 24 hours (hrs) post stimulation (10 – 100ng; Figure 1A – C). The inductions of these pro-inflammatory cytokines by CoV2-S1 were significantly greater than that induced by CoV-S1 (50ng/mL; Figure 1D – F). Higher cytokine inductions by CoV2-S1 were associated with earlier (6hr) and higher NF-κB activation (phospho (p)-p65) compared to that induced by CoV-S1 (Figure 1G).

CoV2-S1-mediated NF-κB activation is dependent on S1-ACE2 interaction.

Immunoprecipitation using anti-His antibody demonstrates that CoV2-S1 / -RBD binding to ACE2 30 minutes post stimulation (Figure 2A). To further assess if CoV2-S1 and ACE2 interaction is required for NF-κB activation, we have designed six antagonistic peptides of varying lengths (AP-1 – 6; 8 – 15 amino acid residues) that were N-terminally biotinylated (Figure 2B). These peptides were designed based on the contact residues on ACE2 in an attempt to inhibit CoV2-S1-ACE2 interaction, including Y449, Y453, L455, F486, N487, Y489, Q493, Q498, T500, N501, G502, and Y505 on CoV2-S1 (Figure 2B; Table 1) (Li et al., 2005; Wang et al., 2020a).

We first screened for abilities of these peptides in reducing p65 phosphorylation by CoV2-S1.

Treatment of BCi-NS1.1 with AP-6, but not AP-1 – 5, reduced p65 phosphorylation levels induced by CoV2-S1 (Figure 2c; 10μM). AP-6 mediated reduction in p65 phosphorylation occurred in a dose-dependent manner (10 – 25μM) with minimal cell death (Figure S1A). Higher dose (50μM) resulted in increased cell death (Figure S1A). We then assessed if AP-6 inhibits S1-ACE2 interaction. In the AP-6 treated group, immunoprecipitation using anti-His antibody also shows reduced CoV2-S1 interaction with ACE2 compared with CoV2-S1-stimulated and non-AP-6-treated group (U; Figure 2E). Conversely, immunoprecipitation

using streptavidin diminished interactions between CoV2-S1 and ACE2 in AP-6 group and not in the non-AP-6-treated group. AP-6 also reduced CoV-S1 and ACE2 interaction, indicating the inhibition potentials of AP-6 across small differences in amino acid residue sequences between CoV2-S1 and CoV-S1 RBM (Figure S1B – C).

This indicates that CoV2-S1 elicits higher inflammatory responses than CoV-S1, and that the CoV2-RBD alone is sufficient for inducing this response. CoV2-S1-ACE2 interaction is required for this heightened inflammatory response.

CoV2-S1-ACE2 facilitates NF-κB activation *via* MAP kinase signalling.

We investigated if S1-mediated production of pro-inflammatory cytokines requires common adaptor proteins MyD88 or TRIF. Knockdown of MyD88 or TRIF inhibited S1-mediated p65 phosphorylation (Figure 3A), indicating MyD88 and TRIF as important signalling adaptors in S1-driven p65 activation. However, immunoprecipitation using anti-His antibody did not pull down MyD88 or TRIF (Figure 3B) 2hrs post stimulation. This indicates an intermediate signalling factor is involved between ACE2 and MyD88/TRIF.

MyD88 and TRIF activates multiple pathways that converge at NF-κB. To determine how CoV2-S1 up-regulates NF-κB activity, we used RT^2 Profiler^{TM} Human Inflammasone PCR array and investigated intracellular signalling pathways involved in NF-κB activation (Figure 3C). CoV2-S1 stimulation in BCi-NS1.1 increased expression of genes involved in NF-κB (*NFKB1, NFKBIA, NFKBIB, RELA, TAB1*) and inflammasome signalling (*NLRP1/3/4/6, AIM2, CASP1, PYCARD, IL1B, and IL18*), but also several factors involved in MAP kinase pathway (*MAPK1/3/3K7/8/9/11/12/13*) (Figure 3D – F; Figure S2).

MAP kinase pathways have been shown to be involved in NF-κB activations (Bergmann et al., 1998; Madrid et al., 2001; Wang et al., 2019; Wesselborg et al., 1997), and consistent with the PCR array. Here CoV2-S1 stimulation in BCi-NS1.1 cells also induced heightened activation of MAP kinase p38 (12 – 24hrs), Erk (2 and 24hrs), and Jnk (24hrs), compared to inductions by CoV-S1 (Figure 4A). Knockdown of p38, Erk or Jnk expressions by siRNAs all resulted in a significant reduction in phosphorylation of p65 following CoV2-S1 treatment (Figure 4B), indicating that the MAP kinase is an important contributor to CoV2-S1-mediated NF-κB activation.

CoV2-S1 stimulates rapid ER stress and UPR that activate NF-κB *via* UPR-MAP kinase crosstalk.

CoV2-S1 induced early activation of Erk, which is a kinase utilised by not only MAP kinase but also ER stress and UPR. ER stress has been shown to be induced by the CoV spike protein (Versteeg et al., 2007). ER-UPR features three main pathways, PERK-Erk-CHOP pathway that modulates apoptosis, ATF6 that regulates protein folding, and the IRE1 – TRAF2 pathway that promotes NF-κB and p38 activation (Pathinayake et al., 2018).

CoV2-S1 and -RBD resulted in an early increase of IRE1 and PERK activations at 2 and 6hrs, respectively, and this was sustained to 24hr post stimulation. Furthermore, IRE1 and PERK activations were higher compared with CoV-S1 and -RBD (Figure 5A). ATF6 activation was equivalent for CoV2-S1 and CoV-S1. As IRE1 activation was induced earlier (2hrs) by CoV2-S1 than MAP kinases, we then investigated if increased ER-UPR by CoV2-S1 leads to heightened MAP kinase activities by siRNAs.

Knockdown of PERK resulted in reduced phosphorylation levels of Erk, but had minimal effect on p65, p38, and Jnk activation (Figure 5B). In contrast, reduction of IRE1 expression decreased p65, p38, and Erk phosphorylation/expression. This indicates that IRE1, and not PERK and ATF6 pathway, is involved in p65 activation.

We also assessed if MAP kinase modulates ER-UPR. While knockdown of either p38, Erk, or Jnk decreased p65 phosphorylation (Figure 4B), reduction of p38 or Erk gene expression led to decreased PERK phosphorylation but not IRE1 activation (Figure 5C). Jnk knockdown led to reduced IRE1 phosphorylation and had no effect on PERK activation. This demonstrates CoV2-S1 promotes NF-κB activation *via* the ER-UPR (IRE1/PERK) and MAP kinase pathway.

CoV2-S1 induces markers of acute bronchial epithelial injury

Acute lung injury is a feature observed with severe COVID-19 (Huang et al., 2020; Lai et al., 2017), and markers associated with epithelial damage IL-1β, TNF, and CCL2 were all markedly increased by CoV2-S1 in our targeted PCR array (Figure 3C), and at protein levels (Figure 1A). CoV2-S1 also significantly up-regulated protein productions of CCL2 in BCi-NS 1.1 cells (Figure 6A). To further investigate if CoV2-S1 induces epithelial damage, we stimulated differentiated primary bronchial epithelial cells (pBECs) cultured at air-liquid interface (ALI) with CoV2-S1 (50 and 100ng). Stimulation resulted in a significant reduction

in transepithelial electrical resistance (TEER; Figure 6B), demonstrating an increased epithelial permeability and tight junction disruption caused by CoV2-S1. This is accompanied with increased protein production of epithelial damage factors IL-1β, TNF, and CCL2, in a CoV2-S1 dose-dependent manner (Figure 6C – E).

Immunofluorescent staining of a tight junction protein zonula occludens-1 (ZO-1) showed strong localisation at the cell borders in the non-stimulated controls, whereas CoV2-S1 led to partial disappearance of ZO-1 at the cell borders (Figure 6F). This indicates that CoV2-S1 may also disrupt epithelial barrier function.

CoV2-S1-antagonistic AP-6 and FDA-approved ER stress and MAP kinase inhibitors ameliorate CoV2-mediated inflammatory response.

CoV2-S1 induced NF-κB activation and subsequent production of pro-inflammatory cytokines was dependent on ACE2 interaction and early ER-UPR and MAP kinase activities. We therefore assessed whether CoV2-S1-mediated inflammation could be reduced by our CoV2-S1 inhibitory peptide AP-6, or with existing FDA-approved pharmacological inhibitors, that target ER stress (4-PBA) or MAP kinase (trametinib and ulixertinib).

Treatment with AP-6 led to a significant decrease in CoV2-S1-mediated phosphorylation of p65 (Figure 2C) and production of IL-6, IL-1β, TNF, but not CCL2 (Figure 7A – D) in a dose-dependent manner. Similarly, the ER stress inhibitor 4-PBA and both MAP kinase inhibitors led to decreased activation of p65 (Figure S3) and expression of these pro-inflammatory and epithelial injury cytokines (Figure 7E – L). These drugs had no effect on non-CoV2-S1-stimulated controls (Figure S4). CoV2-S1-induced reduction in barrier integrity and ZO-1 was prevented *via* treatment with AP-6 and FDA-approved inhibitors, suggesting maintained barrier function (Figure S5A – B). This strongly indicates that AP-6 could serve as a proof-of-concept therapeutic peptides against SARS-CoV-2 and also that ER stress / MAP kinase inhibitors could be used to reduce inflammation and lung injury caused by CoV2-S1.

Discussion

CoV Spike protein and host ACE2 interaction is a critical first step to viral replication and diseases. Here we demonstrate that CoV2 S1 subunit and RBD induces early ER-UPR and MAP kinase activations, leading to hyper-inflammatory responses. Our results indicate that

this inflammatory storm, and downstream consequences are inhibited by S1-inhibitory peptides and existing FDA-approved ER stress and MAP kinase inhibitors (Figure 8).

COVID-19 has been shown to be associated with increased plasma levels of pro-inflammatory cytokines including IL-6 and TNF (Huang et al., 2020; McGonagle et al., 2020; Mehta et al., 2020). SARS-CoV-2 S1 and RBD alone induced heightened levels of IL-6, TNF and IL-1β, and the productions of which were higher compared with CoV-S1. This induction occurs in an ACE2-dependent manner, and the higher affinity of CoV2-S1 towards ACE2 may have contributed to this elevated inflammatory response (Wang et al., 2020a). CoV2-S1-mediated NF-κB activation is also dependent on common TLR adaptor proteins MyD88 and TRIF, although we could not detect interactions between ACE2 and these adaptor proteins. It is possible that CoV2-S1-ACE2 interaction triggers MyD88 and TRIF activations *via* other signalling factors that then result in NF-κB activation.

Our data strong indicates that inflammation could be triggered by CoV2-S1 even before viral replication occurs or in the absence of viral replication. As CoV2-S1 is present throughout viral replication cycles and infection, our data demonstrate that spike proteins are likely to be a major contributor to inflammation. The constant presence of S1 is consistent with the high viral load and a long virus-shedding period observed in patients with severe COVID-19 (Liu et al., 2020). Furthermore, CoV2 spike protein has an estimated half-life of 30 hours in mammalian systems (*in silico* analysis by ExPASy ProtParam) and consists of amino acid residues with long half-lives (leucine (8%), threonine (7.6%), valine (7.6%), alanine (6.2%), glycine (6.4%), and proline (4.6%)). This may suggest persistent presence of CoV2 spike protein from live and dead viruses that plays major role in triggering the inflammatory storm in COVID-19. Importantly, our antagonistic peptide inhibited this binding event and reduced the production of pro-inflammatory cytokines. While peptide sequence optimisations are required to further increase effectiveness and stability, this highlights the potentials of using S1 antagonistic peptides as neutralising molecules against SARS-CoV-2.

The ER is mainly involved in protein folding, trafficking and post-translational modification of secreted and transmembrane proteins (Pathinayake et al., 2018). Viral infections and inflammatory cytokines result in high ratio of misfolded or unfolded proteins in the ER, leading to UPR (Oslowski and Urano, 2011). This adaptive mechanism triggers a range of different innate immune responses *via* different UPR pathways; PERK-Erk-CHOP pathway

that halts protein translation (Harding et al., 2000); ATF6 that facilitates protein folding as well as NF-κB activation (Shen et al., 2005); and IRE1 promotes NF-κB phosphorylation and inflammation (Urano et al., 2000). Here we showed that both ER-UPR and MAP kinases modulate CoV2-S1-induced NF-κB activations.

CoV2-S1 caused early activation of ER-UPR IRE1 and PERK-Erk, leading to MAP kinases phosphorylations, which then facilitated NF-κB-mediated production of pro-inflammatory cytokines. Although IRE1 activation occurred earlier than other ER-UPR and MAP kinase factors, it is likely that CoV2-S1 can promote NF-κB activation *via* ER-UPR and MAP kinase both independently and cooperatively (Bergmann et al., 1998; Madrid et al., 2001; Wesselborg et al., 1997) (Harding et al., 2000; Urano et al., 2000). Our result is consistent with previous reports that showed ER stress and MAP kinase activation by SARS-CoV infection (Lee et al., 2004; Mizutani et al., 2004; Versteeg et al., 2007), we cannot rule out the possibilities of other mechanisms of ER-UPR and MAP kinase activations by CoV2-S1. Furthermore, during SARS-CoV-2 infection, viral RNAs will also trigger inflammatory responses *via* multiple pattern recognition receptors including TLRs and RLRs. This together with spike proteins may instigate more exaggerated inflammatory responses during SARS-CoV-2 infection.

Acute lung injury is a feature of severe COVID-19 (Huang et al., 2020; McGonagle et al., 2020; Mehta et al., 2020). Surprisingly we found that CoV2-S1 and -RBD alone was also sufficient to reduce epithelial barrier function through the release of IL-1β, TNF, and CCL2. Pro-inflammatory cytokines IL-1β and TNF have been shown to induce epithelial damage by further promoting p38 and NF-κB activation (Al-Sadi et al., 2013; Kimura et al., 2013; Kimura et al., 2009; Kolb et al., 2001; Sheridan et al., 1997). CCL2 is a chemokine that has been shown to be transcriptionally driven by NF-κB and is typically released by injured tissues and attracts macrophages to the site of infection and inflammation (Kavandi et al., 2012; Lai et al., 2017).

While CoV2-S1 increased membrane permeability that was consistent with small loss of ZO-1 localisation at cell-cell junctions, it is likely that increased production of these inflammatory and injury-related factors from epithelial cells recruit macrophages to the site of infection, which then promote excessive tissue damage. These inflammatory and injury-stimulated factors as well as macrophages have been reported to be highly elevated in those

with severe COVID-19 (Huang et al., 2020; McGonagle et al., 2020; Mehta et al., 2020), further indicating that this "inflammatory injury" can be driven by CoV2-S1 in severe COVID-19, and may be the first step to ARDS.

Increased ER-UPR and MAP kinase activities as well as pro-inflammatory responses induced by CoV2-S1 could be substantially reduced by FDA-approved ER stress inhibitor 4-PBA and MAP kinase inhibitors trametinib and ulixertinib. 4-PBA is a chemical chaperone currently used for treatment of urea cycle disorder (Lichter-Konecki et al., 2011), and has been used in clinical trials for diabetes (Ozcan et al., 2006), cystic fibrosis (Ozcan et al., 2006), sickle cell disease (Collins et al., 1995), and neurodegenerative diseases (Mimori et al., 2012). Trametinib is a MAP kinase inhibitor used for melanoma (Hoffner and Benchich, 2018), and ulixertinib is a highly potent, selective, reversible, ERK1/2 inhibitor used as cancer treatment (Sullivan et al., 2018). Re-purposing these drugs that has a well-documented safety profile in humans could expedite rapid deployment of these drugs for severe COVID-19.

Collectively, CoV2-S1 induced heightened production of inflammatory cytokines that are primarily driven by MAP kinase and ER stress cross-talks. CoV2-S1 AP-6 demonstrates the feasibility of this proof-of-concept CoV-specific antiviral strategy. While antiviral drugs and vaccines are being developed and assessed, existing FDA-approved ER stress and MAP kinase inhibitors could be immediately deployed in clinical trials as a potential treatment options for those with severe COVID-19.

Acknowledgments

This study is funded by University of Newcastle Faculty Pilot Grant (1032380) and John Hunter Hospital Charitable Trust (G1700465).

The authors have declared that no conflict of interest exists.

Author Contributions

Conceptualization, A. C-Y. H.; Methodology, A. C-Y. H., G. W., A. T. R., P. C. V., P. S.P.; Investigation, A. C-Y. H., G. W., K. D., A. T. R., P. C. V.; Validation, G. W., A. T. R., P. C. V., P. S.P., K. D.; Writing – Original and finalised version, A. C-Y. H.; Writing – Review & Editing, A. C-Y. H., G. W., A. T. R., P. C. V., P. S.P., K. D., J. C. H., F. W., P. A. W.; Funding Acquisition, A. C-Y. H.; F. W.

Declaration of Interests

The authors declare no competing interests.

Figure legends

Figure 1. CoV2-S1 and -RBD stimulated higher productions of IL-6, IL-1β and TNF compared with CoV-S1 and -RBD.

A-C. Protein levels of IL-6, IL-1β and TNF stimulated by SARS-CoV-2 spike subunit 1 (CoV2-S1) and receptor binding domain (RBD) 24hrs post stimulation. **D-F.** Stimulation and comparison of IL-6, IL-1β and TNF by CoV2-S1 and CoV-S1. **G.** Immunoblot (left) and densitometry (right) of induction kinetics of phospho(p)-p65 at 2, 6, 12, and 24hr post stimulation by CoV2-S1 and CoV-S1 compared with CoV2-S1 stimulated but untreated control (U). N = 6 showing mean ± SEM. Immunoblots shown are representative of three independent experiments and β-actin was detected to show equal protein input (lower panel). * $P \leq 0.05$ versus untreated control.

Figure 2. CoV2-S1-mediated NF-κB activation requires ACE2 interaction and can be inhibited by antagonistic peptides.

A. Immunoblot of ACE2 after immunoprecipitation using anti-His antibody 30 minutes post CoV2-S1/-RBD or CoV-2-S1/-RBD stimulation. **B.** Schematic representation of CoV2-S1 protein and peptide design coverage. **C.** Immunoblot of p-p65 and p65 24hrs post CoV2-S1 stimulation and CoV2-S1 antagonistic peptides (AP-1 – 6) compared with untreated control (U). **D.** Immunoblot (left) and densitometry (right) of p-p65 and p65 at 24hrs post CoV2-S1 and AP-6 (10, 25μM) treatment compared with CoV2-S1 stimulated but untreated control (U). **E.** Immunoblot of ACE2 and His following immunoprecipitation using anti-His antibody 30 minutes post CoV2-S1/AP-6 treatment. Immunoblot of His and ACE2 following immunoprecipitation using streptavidin-coupled Dynabeads 30 mintures post CoV2-S1/AP-6 treatment. N = 3 showing mean ± SEM. Immunoblots shown are representative of three independent experiments and β-actin was detected to show equal protein input (lower panel). * $P \leq 0.05$ versus untreated control.

Figure 3. CoV2-S1 stimulates NF-κB activation via MyD88/TRIF adaptors and MAP kinase pathway.

A. Immunoblots of p-p65 phosphorylation 24hrs post CoV2-S1 stimulation in MyD88 and TRIF silenced BCi-NS1.1. **B.** Immunoblots of MyD88 and TRIF after immunoprecipitation using anti-His antibody 2 hours post stimulation. **C-F.** CoV2-S1-stimulated BCi-NS1.1 cells (24hrs) were subjected to RT^2 Profiler™ Human Inflammasone PCR array with highly up-regulated genes involved in NF-κB, Inflammasome, and MAP kinase pathways. N = 3 for Figure 3A-B. Immunoblots shown are representative of three independent experiments and β-actin was detected to show equal protein input (lower panel).

Figure 4. CoV2-S1 mediates NF-κB activation *via* MAP kinase pathways.

A. Immunoblot (top) and densitometry (bottom) of induction kinetics of p-p38, p38, p-Erk, Erk, p-Jnk and Jnk at 2, 6, 12, and 24hr post stimulation by CoV2-S1 and CoV-S1 compared with untreated control (U). **B.** Immunoblots of p-p65, p65, p-p38, p38, p-Erk, Erk, p-Jnk and Jnk 24hrs post CoV2-S1 or -RBD stimulation in p38, Erk or Jnk silenced BCi-NS1.1. N = 3. Immunoblots shown are representative of three independent experiments and β-actin was detected to show equal protein input (lower panel). * $P \leq 0.05$ versus untreated control.

Figure 5. CoV2-S1 induces rapid ER-UPR that activate NF-κB *via* ER-MAP kinase crosstalk.

A. Immunoblot (top) and densitometry (bottom) of induction kinetics of p-IRE1□, IRE1□, p-ATF6, ATF6, p-PERK and PERK at 2, 6, 12, and 24hr post stimulation by CoV2-S1 and CoV-S1 compared with untreated control (U). **B.** Immunoblots of p-p65, p65, p-p38, p38, p-Erk, Erk, p-Jnk, Jnk, IRE1□ and PERK 24hrs post CoV2-S1 or -RBD stimulation in PERK and IRE1□ silenced BCi-NS1.1. **C.** Immunoblots of p-PERK and p-IRE1□ post CoV2-S1 or -RBD stimulation in p38, Erk or Jnk silenced BCi-NS1.1. N = 3. Immunoblots shown are representative of three independent experiments and β-actin was detected to show equal protein input (lower panel). * $P \leq 0.05$ versus untreated control.

Figure 6. CoV2-S1 promotes epithelial damage.

A. CCL2 protein production at 24hrs post CoV2-S1 stimulation in BCi-NS1.1. **B.** Percentage changes in transepithelial electrical resistance (TEER) in differentiated primary bronchial epithelial cells (pBECs) cultured at air-liquid interface (ALI) 24hrs post CoV2-S1 stimulation. **C-E.** Protein levels of IL-1β, TNF□, and CCL2 at 24hrs post CoV2-S1

412 stimulation in pBECs-ALI. N = 3. * $P \leq 0.05$ versus untreated control. **F.** Immunofluorescent
413 images of ZO-1 labelling. N = 2.
414
415 **Figure 7. CoV2-S1 antagonistic peptide AP-6 and FDA-approved ER stress and MAP**
416 **kinase inhibitors suppress CoV2-S1-mediated production of pro-inflammatory**
417 **cytokines.**
418 **A-D.** Protein levels of IL-6, IL-1β and TNF at 24hrs post stimulation by CoV2-S1 and
419 treatment with antagonistic peptide AP-6, **E-H.** 4-PBA, and **I-L.** Trametinib, and Ulixertinib.
420 N = 3. * $P \leq 0.05$ versus untreated control.
421
422 **Figure 8. Schematics of CoV2-S1-mediated inflammation via ER-UPR and MAP kinase**
423 **pathways.**
424 SARS-CoV-2 (CoV2) spike protein binds with ACE2 on the surface of human bronchial
425 epithelial cells and rapidly facilitates the induction of ER stress and unfolded protein
426 response (UPR). Activation of UPR (PERK and IRE1) promotes the activation of MAP
427 kinases, and the two pathways synergistically drive the activation of NF-κB and production
428 of pro-inflammatory cytokines. FDA-approved ER-UPR inhibitor 4-phenylburic acid (4-
429 PBA) and MAP kinase inhibitors (trametinib and ulixertinib) suppressed CoV2-S1-induced
430 ER stress and MAP kinase activities, resulting in reduced NF-κB-mediated expression of pro-
431 inflammatory cytokines.
432
433 **STAR Methods**
434 **Experimental model and subject details**
435 Cell line
436 BCi-NS1.1 cells were obtained from Prof. Ronald Crystal Laboratory at Weill Cornell
437 Medical College, and Memorial Sloan-Kettering Cancer Center, New York, NY, USA)
438 (Walters et al., 2013). The cells were cultured in hormone supplemented Bronchial Epithelial
439 Cell Growth Media (BEGM; Lonza, Switzerland) supplemented with 50U/mL penicillin and
440 streptomycin (Hayman et al., 2019; Hu et al., 2019; Kedzierski et al., 2017).
441
442 Human subject recruitment for pBECs
443 Five healthy control subjects were recruited for bronchoscopy. Healthy non-smoking controls
444 with no evidence of airflow obstruction, bronchial hyper-responsiveness to hypertonic saline
445 challenge, or chronic respiratory symptoms were also recruited. Clinical history, examination

and spirometry were performed on all individuals, whom were also questioned about the previous severity of cold symptoms. At the time of recruitment none of the subjects had symptoms of acute respiratory tract infections for the preceding four weeks and did not have a diagnosis of lung cancer.

All subjects gave written informed consent. All procedures were performed according to approval from The University of Newcastle Human Ethics Committees

Differentiation of primary bronchial epithelial cells (pBECs) at air-liquid-interface (ALI)

Human pBECs were obtained by endobronchial brushing and research bronchoscopy in accordance with standard guidelines. pBECs were cultured in BEGM in polycarbonate tissue culture flasks as previously described (Hsu et al., 2011; Hsu et al., 2017; Hsu et al., 2012; Hsu et al., 2016; Hsu et al., 2015; Kedzierski et al., 2017; Parsons et al., 2014; Vanders et al., 2019), and were then cultured on polyester membrane transwells (12mm diameter, 0.4µM pore size, Corning, USA) under submerged condition in ALI initial media (31.25mL low glucose DMEM and BEGM, 1µL of 1mM All-trans retinoic acid, 4µL of 25µg/mL recombinant human epidermal growth factor (rhEGF), 62.5µL hydrocortisone, bovine insulin, epinephrine, transferrin, 80µM ethanolamine, 0.3mM MgCl2, 0.4mM MgSO4, 0.5mg/mL BSA, and 250µL bovine pituitary extract, supplemented with penicillin/streptomycin and amphotericin B). When cells become fully confluent, pBECs were air-lifted by removing apical media and changing basal media into ALI final media (as described above for ALI initial media but with 0.5ng/mL of rhEGF). Transepithelial resistance (TEER) was measured every seven days using a EVOM2 Epithelial Voltohmmeter (World Precision Instruments, USA). The basal media was replaced with fresh ALI final media every second day. pBECs were cultured at ALI for 25 days and then used for experiments. All cells were cultured and maintained at 37°C / 5% CO_2.

Method details

Spike protein subunit 1 (S1) and receptor binding domain (RBD) stimulation

For cells cultured in submerged and at ALI conditions, his-tagged S1 and RBD (Sino Biological Inc.) was diluted in BEBM minimal media (Lonza, Switzerland) and added to the cells. For pBECs at ALI, S1 and RBD was added to the apical side.

CoV2-S1 antagonistic peptides

Six peptides of varying lengths (8 – 15 amino acid residues) were designed based on the amino acid residues critical in ACE2 binding within the receptor binding motif (RBM) of the receptor binding domain (RBD). The peptides were biotinylated at the amino-terminus with carboxy-terminal amidation. The peptides were synthesised by GenScript Biotech Corp. The peptides were added to the BCi-NS1.1 at 10 or 25µM, or added to pBECs-ALI (25µM) at the apical side.

Drugs

ER stress inhibitor 4-phenylburic acid (4-PBA) was purchased from Sigma-Aldrich, and resuspended in H_2O and diluted in culture media. MAP kinase inhibitors trametinib (GSK1120212) and ulixertinib (BVD-523) were purchased from Selleck Chemicals and were resuspended and diluted in DMSO.

Cell viability

Cell viability was measured using PE Annexin V Apoptosis Detection kit I (Becton Dickinson) according to manufacturer's instruction. Cells were stained with annexin V-PE and vital dye 7-amino-actinomycin (7-AAD), and then analyzed using a FACSCanto II (Becton Dickinson) and FACSDiva software. Viable cells were stained AxV negative / 7-AAD negative and expressed as percentage of total analyzed cells.

siRNAs

siRNAs specific to MyD88, TRIF, p38, Erk, Jnk, PERK, and IRE1 (Life Technologies, USA) were reverse transfected into cells using siPORT NeoFX transfection agent (Ambion, USA) according to manufacturer's instruction. Silence Negative controls (Life Technologies, USA) were used as siRNA negative controls.

PCR array

RNAs from S1-stimulated cells were extracted using RNeasy Mini Kits and QIAcube (Qiagen, USA) according to manufacturer's instruction. 200ng of RNAs were reverse transcribed to cDNA using random primers (Applied Biosystem, USA). cDNAs were then subjected to pathway-focused gene expression array using RT^2 Profiler^{TM} Human Inflammasome PCR array (Qiagen, USA). The raw data was analysed by the Data Analysis Center on Qiagen website (https://www.qiagen.com/mx/shop/genes-and-pathways/data-analysis-center-overview-page/).

Immunoblotting and immunoprecipitation

S1-stimulated cells were lysed in protease-inhibitor cocktail supplemented RIPA buffer (Roche, UK). Proteins were subjected to SDS-PAGE (Bio-Rad Laboratories, USA) and transferred onto polyvinylidene fluoride membranes (Merck-Milipore, USA). Proteins were detected using antibodies to His, MyD88, TRIF, p65, phospho-(p)-p65, p38, p-p38, Erk, p-Erk, Jnk, p-Jnk, PERK, p-PERK, IRE1□, and p-IRE1□ antibodies (All from Abcam, UK). Antibody to ACE2 was obtained from RnD Systems (USA). For immunoprecipitation, whole cell lysates (1mg) were immunoprecipitated using anti-His antibody or isotytpe antibody (Abcam, UK), streptavidin-coupled Dynabeads™ M-280 and Dynabeads™ His-tag isolation & Pulldown kit (Life Technologies, USA) according to manufacturer's instruction. Proteins were detected using SuperSignal WestFemto Maximum Sensitivity Substrate (Thermo Fisher Scientific, USA) and visualised on a ChemiDoc MP Imaging system (Bio-Rad Laboratories, USA).

Immunofluorescent microscopy

Treated pBECs cultured at ALI were fixed 4% paraformaldehyde and blocked with 50mM glycine overnight, and then stained with anti-ZO-1 antibody (Thermo Fisher Scientific, USA) or rabbit isotype IgG (Abcam, UK), counter stained with DAPI (Life Technologies, USA), and viewed under a Axio Imager M2 microscope and analyzed using Zen imaging software (Zeiss) as described previously (Liu et al., 2019; Liu et al., 2016; Liu et al., 2017; Reid et al., 2020).

Cytometric bead array and ELISA

Human IL-6, IL-1β, and TNF□ concentrations were determined by cytometric bead array and flow cytometry (FACSCanto II flow cytometer; BD Biosciences, USA) according to the manufacturer's instructions. Human CCL2 and TGFβ was measured by ELISA according to the manufacturer's instructions (R&D Systems, USA).

Quantification and statistical analysis

Statistical analysis

Data were analysed on GraphPad Prism 8. Statistical significance of differences was assessed using parametric Student's two tailed t test for normally distributed data and Mann-Whitney U test for non-parametric data. Differences were considered significant when $p < 0.05$.

Figure S1. AP-6 reduces CoV-S1 and ACE2 interaction.

A. Cell viability measured by annexin-V/7-AAD staining and flow cytometry. **B.** Immunoblot of ACE2 and His following immunoprecipitation using anti-His antibody 30 minutes post CoV2-S1/AP-6 treatment. N = 3. Immunoblots shown are representative of three independent experiments. **C.** Amino acid residue sequence alignments of CoV2-S1 and CoV-S1. Blue = AP-6 contact region. Sequence alignment performed by Clustal Omega.

Figure S2. CoV2-S1 up-regulates genes involved in inflammation, inflammasome and MAP kinase pathways.

CoV2-S1-stimulated BCi-NS1.1 cells were subjected to RT^2 Profiler™ Human Inflammasone PCR array with highly up-regulated genes involved in NF-κB, Inflammasome, and MAP kinase pathways. N=3.

Figure S3. CoV2-S1 antagonistic peptides, Trametinib, and Ulixertinib had no effect on IL-6, IL-1β, TNF, and CCL2 productions in non-CoV2-S1-treated cells.

Protein levels of IL-6, IL-1β, TNF, and CCL2 induced by **A-D** antagonistic peptide (AP-6), **E-H.** 4-PBA, **I-L.** trametinib, and **M-P.** ulixertinib. N = 3.

Figure S4. FDA-approved ER stress and MAP kinase inhibitors suppress CoV2-S1-mediated NF-κB activation.

Immunoblot (top) and densitometry (bottom) of p-p65 and p65 at 24hr post stimulation by CoV2-S1 or -RBD compared with vehicle control. Immunoblots shown are representative of three independent experiments and β-actin was detected to show equal protein input (lower panel).

Figure S5. AP-6, 4-PBA, trametinib and ulixertinib improves epithelial permeability.

A. Percentage changes in transepithelial electrical resistance (TEER) in differentiated primary bronchial epithelial cells (pBECs) cultured at air-liquid interface (ALI) at 24hrs post CoV2-S1 stimulation and treatment with either AP-6, 4-PBA, trametinib, and ulixertinib. N = 3. * $P \leq 0.05$ versus non-CoV2-S1-stimulated control, + versus CoV2-S1-stimulated group. **B.** Immunofluorescent images of ZO-1 staining. N = 2.

References

Al-Sadi, R., Guo, S., Ye, D., Dokladny, K., Alhmoud, T., Ereifej, L., Said, H.M., and Ma, T.Y. (2013). Mechanism of IL-1beta modulation of intestinal epithelial barrier involves p38 kinase and activating transcription factor-2 activation. J Immunol 190, 6596-6606

Alexopoulou, L., Holt, A.C., Medzhitov, R., and Flavell, R.A. (2001). Recognition of double-stranded RNA and activation of NF-kappaB by Toll-like receptor 3. Nature 413, 732-738

Bergmann, M., Hart, L., Lindsay, M., Barnes, P.J., and Newton, R. (1998). IkappaBalpha degradation and nuclear factor-kappaB DNA binding are insufficient for interleukin-1beta and tumor necrosis factor-alpha-induced kappaB-dependent transcription. Requirement for an additional activation pathway. The Journal of biological chemistry 273, 6607-6610

Collins, A.F., Pearson, H.A., Giardina, P., McDonagh, K.T., Brusilow, S.W., and Dover, G.J. (1995). Oral sodium phenylbutyrate therapy in homozygous beta thalassemia: a clinical trial. Blood 85, 43-49

Diebold, S.S., Kaisho, T., Hemmi, H., Akira, S., and Reis e Sousa, C. (2004). Innate antiviral responses by means of TLR7-mediated recognition of single-stranded RNA. Science 303, 1529-1531

Guan, X., Yuan, Y., Wang, G., Zheng, R., Zhang, J., Dong, B., Ran, N., Hsu, A.C., Wang, C., and Wang, F. (2020). Ginsenoside Rg3 ameliorates acute exacerbation of COPD by suppressing neutrophil migration. Int Immunopharmacol 83, 106449

Harding, H.P., Zhang, Y., Bertolotti, A., Zeng, H., and Ron, D. (2000). Perk is essential for translational regulation and cell survival during the unfolded protein response. Molecular cell 5, 897-904

Hayman, T.J., Hsu, A.C., Kolesnik, T.B., Dagley, L.F., Willemsen, J., Tate, M.D., Baker, P.J., Kershaw, N.J., Kedzierski, L., Webb, A.I., *et al.* (2019). RIPLET, and not TRIM25, is required for endogenous RIG-I-dependent antiviral responses. Immunology and cell biology 97, 840-852

Hoffner, B., and Benchich, K. (2018). Trametinib: A Targeted Therapy in Metastatic Melanoma. J Adv Pract Oncol 9, 741-745

Hsu, A.C., Barr, I., Hansbro, P.M., and Wark, P.A. (2011). Human influenza is more effective than avian influenza at antiviral suppression in airway cells. American journal of respiratory cell and molecular biology 44, 906-913

Hsu, A.C., Dua, K., Starkey, M.R., Haw, T.J., Nair, P.M., Nichol, K., Zammit, N., Grey, S.T., Baines, K.J., Foster, P.S., *et al.* (2017). MicroRNA-125a and -b inhibit A20 and MAVS to promote inflammation and impair antiviral response in COPD. JCI Insight 2, e90443

Hsu, A.C., Parsons, K., Barr, I., Lowther, S., Middleton, D., Hansbro, P.M., and Wark, P.A. (2012). Critical role of constitutive type I interferon response in bronchial epithelial cell to influenza infection. PLoS One 7, e32947

Hsu, A.C., Parsons, K., Moheimani, F., Knight, D.A., Hansbro, P.M., Fujita, T., and Wark, P.A. (2016). Impaired Antiviral Stress Granule and IFN-beta Enhanceosome Formation Enhances Susceptibility to Influenza Infection in Chronic Obstructive Pulmonary Disease Epithelium. American journal of respiratory cell and molecular biology 55, 117-127

Hsu, A.C., Starkey, M.R., Hanish, I., Parsons, K., Haw, T.J., Howland, L.J., Barr, I., Mahony, J.B., Foster, P.S., Knight, D.A., *et al.* (2015). Targeting PI3K-p110alpha Suppresses Influenza Virus Infection in Chronic Obstructive Pulmonary Disease. American journal of respiratory and critical care medicine 191, 1012-1023

Hu, M., Schulze, K.E., Ghildyal, R., Henstridge, D.C., Kolanowski, J.L., New, E.J., Hong, Y., Hsu, A.C., Hansbro, P.M., Wark, P.A., *et al.* (2019). Respiratory syncytial virus co-opts host mitochondrial function to favour infectious virus production. Elife 8

Huang, C., Wang, Y., Li, X., Ren, L., Zhao, J., Hu, Y., Zhang, L., Fan, G., Xu, J., Gu, X., *et al.* (2020). Clinical features of patients infected with 2019 novel coronavirus in Wuhan, China. Lancet 395, 497-506

Kavandi, L., Collier, M.A., Nguyen, H., and Syed, V. (2012). Progesterone and calcitriol attenuate inflammatory cytokines CXCL1 and CXCL2 in ovarian and endometrial cancer cells. J Cell Biochem 113, 3143-3152

Kedzierski, L., Tate, M.D., Hsu, A.C., Kolesnik, T.B., Linossi, E.M., Dagley, L., Dong, Z., Freeman, S., Infusini, G., Starkey, M.R., *et al.* (2017). Suppressor of cytokine signaling (SOCS)5 ameliorates influenza infection via inhibition of EGFR signaling. Elife 6

635 Kimura, K., Morita, Y., Orita, T., Haruta, J., Takeji, Y., and Sonoda, K.H. (2013). Protection of
636 human corneal epithelial cells from TNF-alpha-induced disruption of barrier function by rebamipide.
637 Invest Ophthalmol Vis Sci 54, 2572-2760
638 Kimura, K., Teranishi, S., and Nishida, T. (2009). Interleukin-1beta-induced disruption of barrier
639 function in cultured human corneal epithelial cells. Invest Ophthalmol Vis Sci 50, 597-603
640 Kolb, M., Margetts, P.J., Anthony, D.C., Pitossi, F., and Gauldie, J. (2001). Transient expression of
641 IL-1beta induces acute lung injury and chronic repair leading to pulmonary fibrosis. J Clin Invest 107,
642 1529-1536
643 Lai, C., Wang, K., Zhao, Z., Zhang, L., Gu, H., Yang, P., and Wang, X. (2017). C-C Motif
644 Chemokine Ligand 2 (CCL2) Mediates Acute Lung Injury Induced by Lethal Influenza H7N9 Virus.
645 Frontiers in microbiology 8, 587
646 Le Goffic, R., Pothlichet, J., Vitour, D., Fujita, T., Meurs, E., Chignard, M., and Si-Tahar, M. (2007).
647 Cutting Edge: Influenza A virus activates TLR3-dependent inflammatory and RIG-I-dependent
648 antiviral responses in human lung epithelial cells. J Immunol 178, 3368-3372
649 Lee, C.H., Chen, R.F., Liu, J.W., Yeh, W.T., Chang, J.C., Liu, P.M., Eng, H.L., Lin, M.C., and Yang,
650 K.D. (2004). Altered p38 mitogen-activated protein kinase expression in different leukocytes with
651 increment of immunosuppressive mediators in patients with severe acute respiratory syndrome. J
652 Immunol 172, 7841-7847
653 Li, F., Li, W., Farzan, M., and Harrison, S.C. (2005). Structure of SARS coronavirus spike receptor-
654 binding domain complexed with receptor. Science 309, 1864-1868
655 Lichter-Konecki, U., Diaz, G.A., Merritt, J.L., 2nd, Feigenbaum, A., Jomphe, C., Marier, J.F.,
656 Beliveau, M., Mauney, J., Dickinson, K., Martinez, A., *et al.* (2011). Ammonia control in children
657 with urea cycle disorders (UCDs); phase 2 comparison of sodium phenylbutyrate and glycerol
658 phenylbutyrate. Mol Genet Metab 103, 323-329
659 Liu, G., Cooley, M.A., Jarnicki, A.G., Borghuis, T., Nair, P.M., Tjin, G., Hsu, A.C., Haw, T.J.,
660 Fricker, M., Harrison, C.L., *et al.* (2019). Fibulin-1c regulates transforming growth factor-beta
661 activation in pulmonary tissue fibrosis. JCI Insight 5
662 Liu, G., Cooley, M.A., Jarnicki, A.G., Hsu, A.C., Nair, P.M., Haw, T.J., Fricker, M., Gellatly, S.L.,
663 Kim, R.Y., Inman, M.D., *et al.* (2016). Fibulin-1 regulates the pathogenesis of tissue remodeling in
664 respiratory diseases. JCI Insight 1
665 Liu, G., Cooley, M.A., Nair, P.M., Donovan, C., Hsu, A.C., Jarnicki, A.G., Haw, T.J., Hansbro, N.G.,
666 Ge, Q., Brown, A.C., *et al.* (2017). Airway remodelling and inflammation in asthma are dependent on
667 the extracellular matrix protein fibulin-1c. J Pathol 243, 510-523
668 Liu, Y., Yan, L.M., Wan, L., Xiang, T.X., Le, A., Liu, J.M., Peiris, M., Poon, L.L.M., and Zhang, W.
669 (2020). Viral dynamics in mild and severe cases of COVID-19. Lancet Infect Dis
670 Madrid, L.V., Mayo, M.W., Reuther, J.Y., and Baldwin, A.S., Jr. (2001). Akt stimulates the
671 transactivation potential of the RelA/p65 Subunit of NF-kappa B through utilization of the Ikappa B
672 kinase and activation of the mitogen-activated protein kinase p38. The Journal of biological chemistry
673 276, 18934-18940
674 Magagnoli, J., Narendran, S., Pereira, F., Cummings, T., Hardin, J.W., Sutton, S.S., and Ambati, J.
675 (2020). Outcomes of hydroxychloroquine usage in United States veterans hospitalized with Covid-19.
676 medRxiv, 2020.2004.2016.20065920
677 Mahevas, M., Tran, V.-T., Roumier, M., Chabrol, A., Paule, R., Guillaud, C., Gallien, S., Lepeule, R.,
678 Szwebel, T.-A., Lescure, X., *et al.* (2020). No evidence of clinical efficacy of hydroxychloroquine in
679 patients hospitalized for COVID-19 infection with oxygen requirement: results of a study using
680 routinely collected data to emulate a target trial. medRxiv, 2020.2004.2010.20060699
681 McGonagle, D., Sharif, K., O'Regan, A., and Bridgewood, C. (2020). The Role of Cytokines
682 including Interleukin-6 in COVID-19 induced Pneumonia and Macrophage Activation Syndrome-
683 Like Disease. Autoimmun Rev, 102537
684 Mehta, P., McAuley, D.F., Brown, M., Sanchez, E., Tattersall, R.S., Manson, J.J., and Hlh Across
685 Speciality Collaboration, U.K. (2020). COVID-19: consider cytokine storm syndromes and
686 immunosuppression. Lancet 395, 1033-1034
687 Mimori, S., Okuma, Y., Kaneko, M., Kawada, K., Hosoi, T., Ozawa, K., Nomura, Y., and Hamana,
688 H. (2012). Protective effects of 4-phenylbutyrate derivatives on the neuronal cell death and
689 endoplasmic reticulum stress. Biol Pharm Bull 35, 84-90

690 Mizutani, T., Fukushi, S., Saijo, M., Kurane, I., and Morikawa, S. (2004). Phosphorylation of p38
691 MAPK and its downstream targets in SARS coronavirus-infected cells. Biochem Biophys Res
692 Commun 319, 1228-1234
693 Oslowski, C.M., and Urano, F. (2011). Measuring ER stress and the unfolded protein response using
694 mammalian tissue culture system. Methods Enzymol 490, 71-92
695 Ozcan, U., Yilmaz, E., Ozcan, L., Furuhashi, M., Vaillancourt, E., Smith, R.O., Gorgun, C.Z., and
696 Hotamisligil, G.S. (2006). Chemical chaperones reduce ER stress and restore glucose homeostasis in
697 a mouse model of type 2 diabetes. Science 313, 1137-1140
698 Parsons, K.S., Hsu, A.C., and Wark, P.A. (2014). TLR3 and MDA5 signalling, although not
699 expression, is impaired in asthmatic epithelial cells in response to rhinovirus infection. Clin Exp
700 Allergy 44, 91-101
701 Pathinayake, P.S., Hsu, A.C., Waters, D.W., Hansbro, P.M., Wood, L.G., and Wark, P.A.B. (2018).
702 Understanding the Unfolded Protein Response in the Pathogenesis of Asthma. Front Immunol 9, 175
703 Reid, A.T., Nichol, K.S., Chander Veerati, P., Moheimani, F., Kicic, A., Stick, S.M., Bartlett, N.W.,
704 Grainge, C.L., Wark, P.A.B., Hansbro, P.M., *et al.* (2020). Blocking Notch3 Signaling Abolishes
705 MUC5AC Production in Airway Epithelial Cells from Individuals with Asthma. American journal of
706 respiratory cell and molecular biology 62, 513-523
707 Saito, T., and Gale, M., Jr. (2008). Differential recognition of double-stranded RNA by RIG-I-like
708 receptors in antiviral immunity. The Journal of experimental medicine 205, 1523-1527
709 Shen, J., Snapp, E.L., Lippincott-Schwartz, J., and Prywes, R. (2005). Stable binding of ATF6 to BiP
710 in the endoplasmic reticulum stress response. Molecular and cellular biology 25, 921-932
711 Sheridan, B.C., McIntyre, R.C., Meldrum, D.R., and Fullerton, D.A. (1997). Pentoxifylline treatment
712 attenuates pulmonary vasomotor dysfunction in acute lung injury. J Surg Res 71, 150-154
713 Sullivan, R.J., Infante, J.R., Janku, F., Wong, D.J.L., Sosman, J.A., Keedy, V., Patel, M.R., Shapiro,
714 G.I., Mier, J.W., Tolcher, A.W., *et al.* (2018). First-in-Class ERK1/2 Inhibitor Ulixertinib (BVD-523)
715 in Patients with MAPK Mutant Advanced Solid Tumors: Results of a Phase I Dose-Escalation and
716 Expansion Study. Cancer Discov 8, 184-195
717 Urano, F., Wang, X., Bertolotti, A., Zhang, Y., Chung, P., Harding, H.P., and Ron, D. (2000).
718 Coupling of stress in the ER to activation of JNK protein kinases by transmembrane protein kinase
719 IRE1. Science 287, 664-666
720 Vanders, R.L., Hsu, A., Gibson, P.G., Murphy, V.E., and Wark, P.A.B. (2019). Nasal epithelial cells
721 to assess in vitro immune responses to respiratory virus infection in pregnant women with asthma.
722 Respiratory research 20, 259
723 Versteeg, G.A., van de Nes, P.S., Bredenbeek, P.J., and Spaan, W.J. (2007). The coronavirus spike
724 protein induces endoplasmic reticulum stress and upregulation of intracellular chemokine mRNA
725 concentrations. Journal of virology 81, 10981-10990
726 Walters, M.S., Gomi, K., Ashbridge, B., Moore, M.A., Arbelaez, V., Heldrich, J., Ding, B.S., Rafii,
727 S., Staudt, M.R., and Crystal, R.G. (2013). Generation of a human airway epithelium derived basal
728 cell line with multipotent differentiation capacity. Respiratory research 14, 135
729 Wang, G., Pang, Z., Chen-Yu Hsu, A., Guan, X., Ran, N., Yuan, Y., Wang, Z., Guo, Y., Zheng, R.,
730 and Wang, F. (2019). Combined treatment with SB203580 and dexamethasone suppresses non-
731 typeable Haemophilus influenzae-induced Th17 inflammation response in murine allergic asthma.
732 European journal of pharmacology 862, 172623
733 Wang, J.P., Bowen, G.N., Padden, C., Cerny, A., Finberg, R.W., Newburger, P.E., and Kurt-Jones,
734 E.A. (2008). Toll-like receptor-mediated activation of neutrophils by influenza A virus. Blood 112,
735 2028-2034
736 Wang, Q., Zhang, Y., Wu, L., Niu, S., Song, C., Zhang, Z., Lu, G., Qiao, C., Hu, Y., Yuen, K.Y., *et*
737 *al.* (2020a). Structural and Functional Basis of SARS-CoV-2 Entry by Using Human ACE2. Cell
738 Wang, X., Xu, W., Hu, G., Xia, S., Sun, Z., Liu, Z., Xie, Y., Zhang, R., Jiang, S., and Lu, L. (2020b).
739 SARS-CoV-2 infects T lymphocytes through its spike protein-mediated membrane fusion. Cell Mol
740 Immunol
741 Wesselborg, S., Bauer, M.K., Vogt, M., Schmitz, M.L., and Schulze-Osthoff, K. (1997). Activation of
742 transcription factor NF-kappaB and p38 mitogen-activated protein kinase is mediated by distinct and
743 separate stress effector pathways. The Journal of biological chemistry 272, 12422-12429

744 Zhou, P., Yang, X.L., Wang, X.G., Hu, B., Zhang, L., Zhang, W., Si, H.R., Zhu, Y., Li, B., Huang,
745 C.L., *et al.* (2020). A pneumonia outbreak associated with a new coronavirus of probable bat origin.
746 Nature 579, 270-273

747

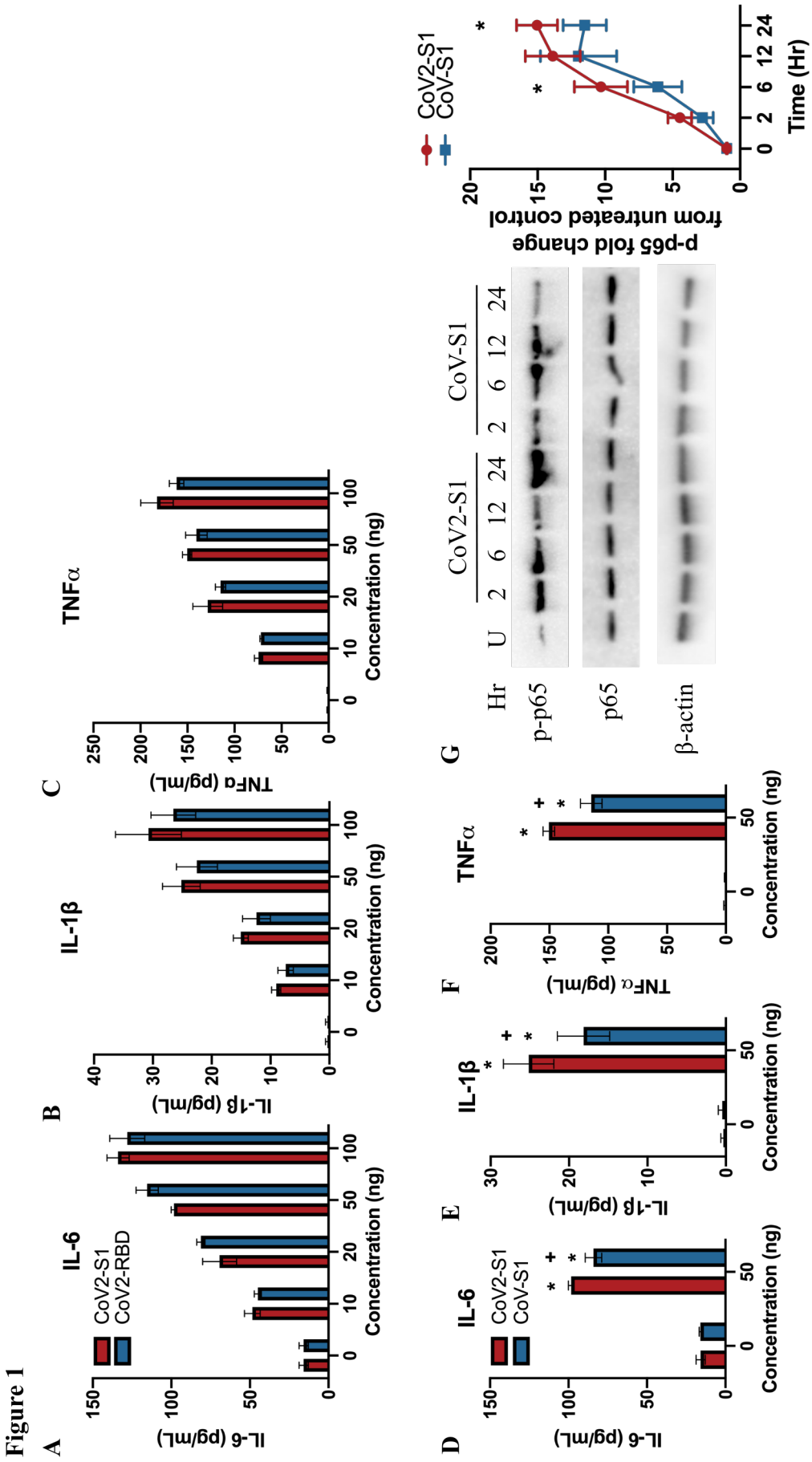

Figure 2

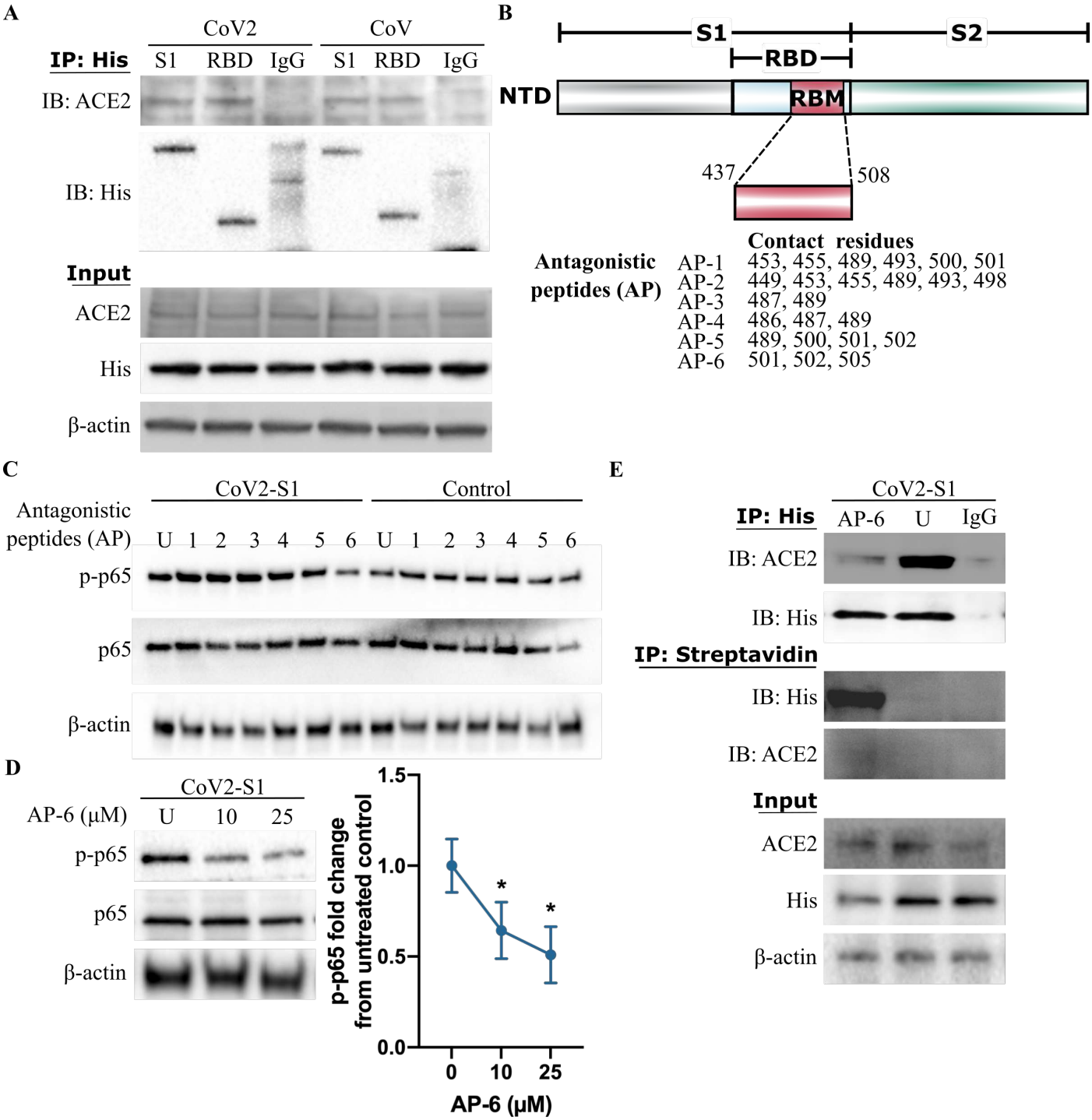

Figure 3

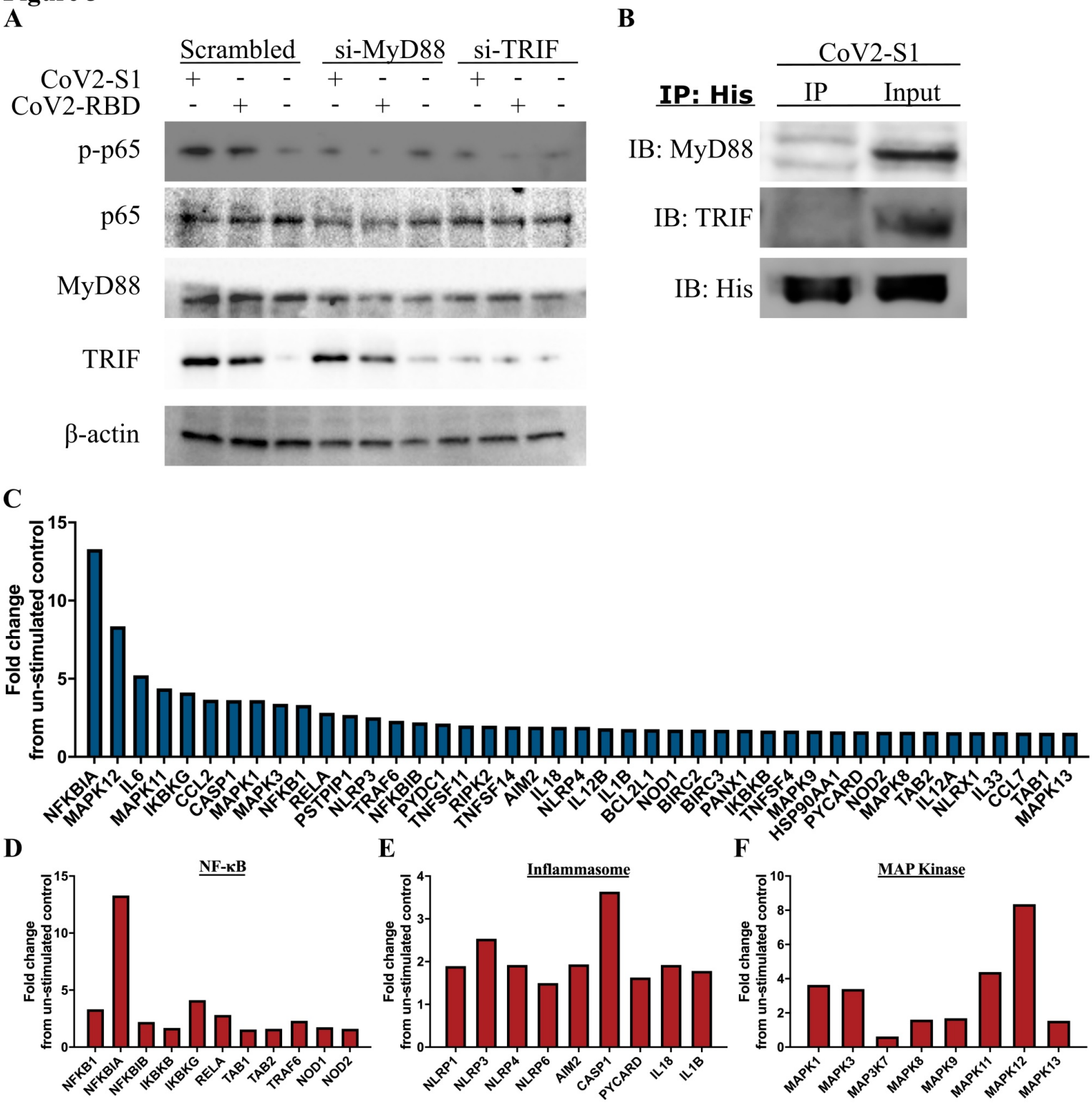

Figure 4

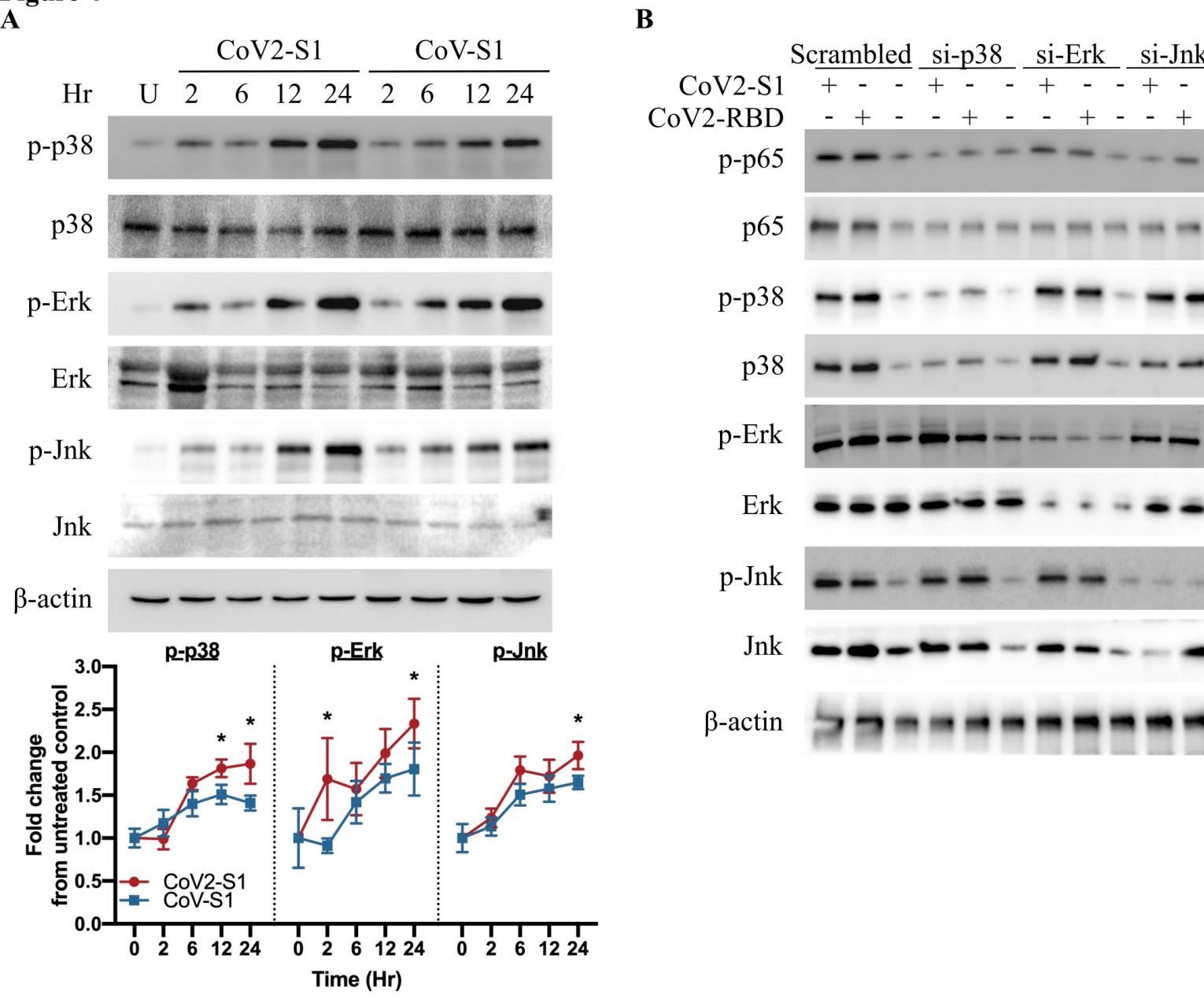

Figure 5

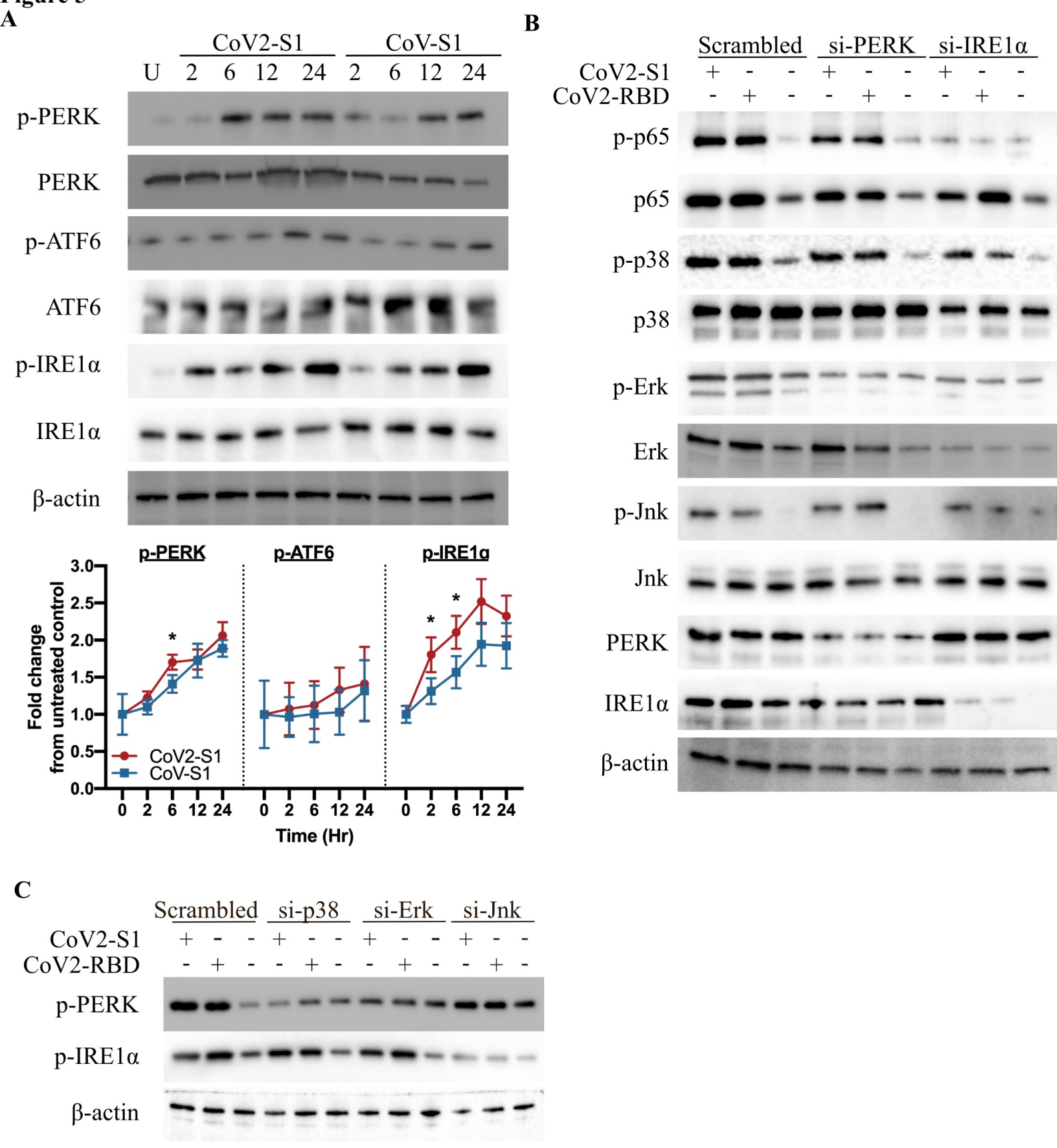

Figure 6

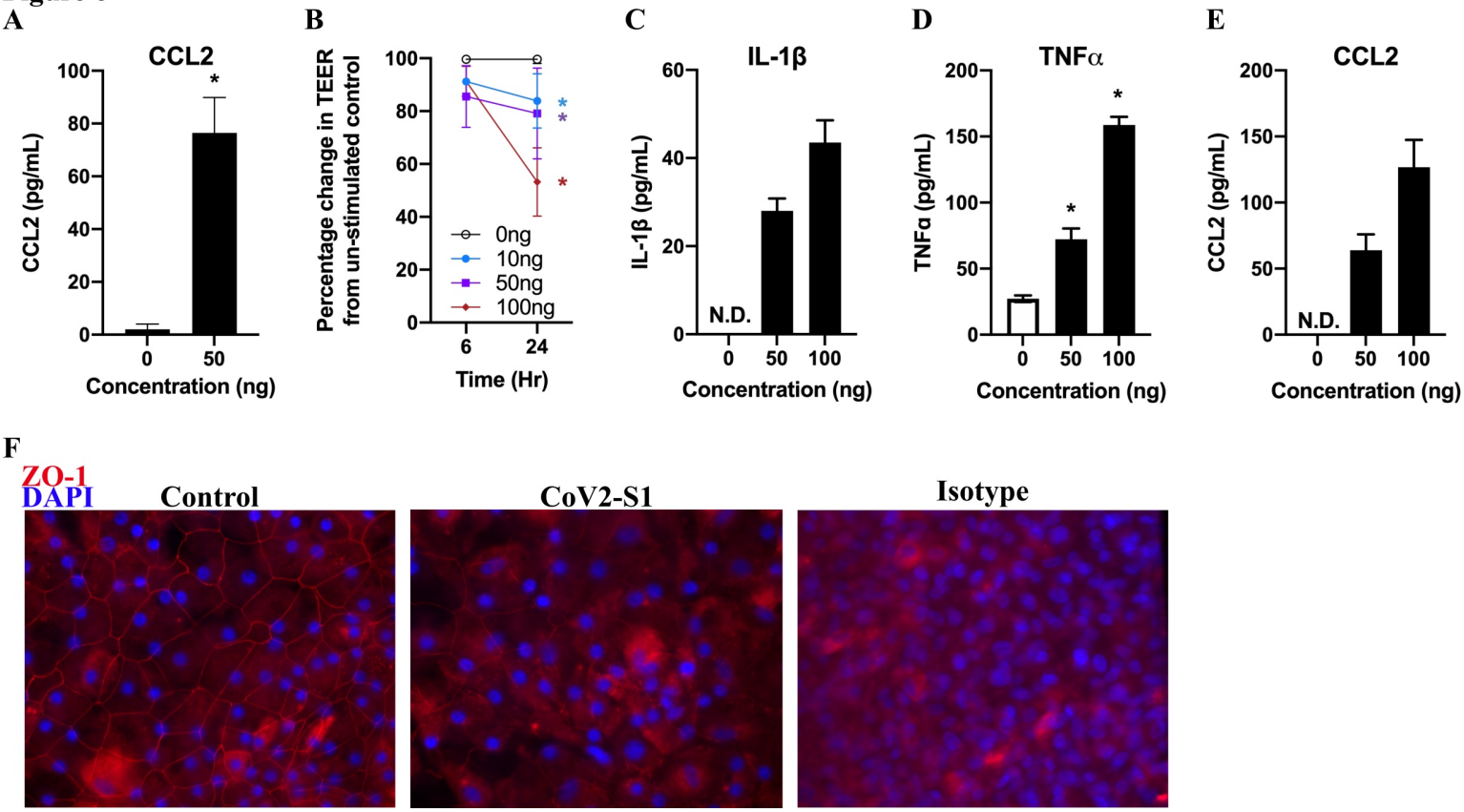

F

Figure 7

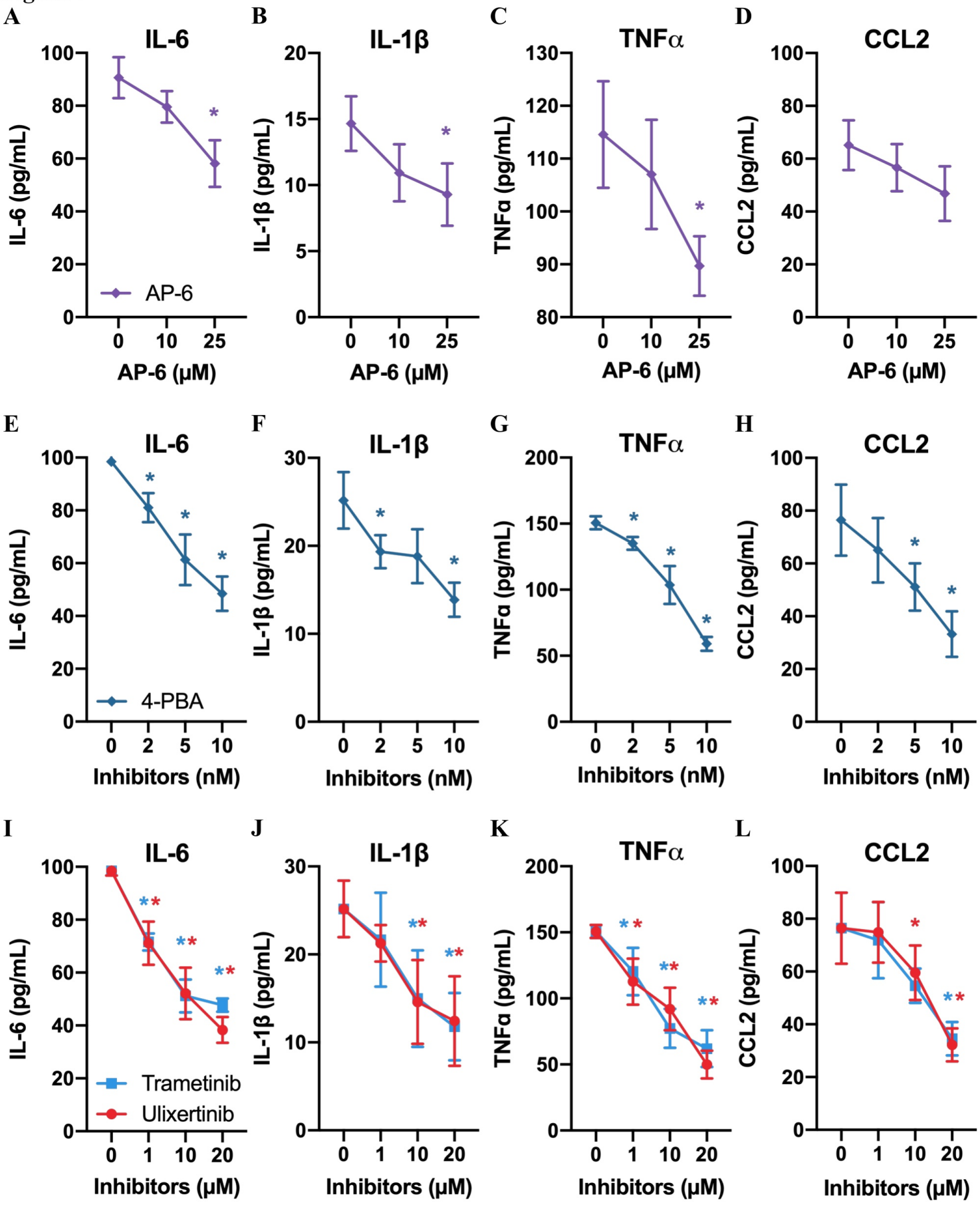

Figure 8